lncRNA Colorectal Neoplasia Differentially Expressed (CRNDE) Promotes Proliferation and Inhibits Apoptosis in Non-Small Cell Lung Cancer Cells by Regulating the miR-641/CDK6 Axis

Authors' Contribution:
Study Design A
Data Collection B
Statistical Analysis C
Data Interpretation D
Manuscript Preparation E
Literature Search F
Funds Collection G

ABCE Ya-Feng Fan
BCE   Zhong-Ping Yu
BE   Xiao-Yan Cui

Department Three of Respiratory Medicine, Shanxi Provincial Cancer Hospital, Taiyuan, Shanxi, P.R. China

Corresponding Author: Ya-Feng Fan, e-mail: bg550004@126.com
Source of support: Departmental sources

Background: The lncRNA Colorectal Neoplasia Differentially Expressed (CRNDE) gene has been reported as a potential oncogene in NSCLC. Nevertheless, the molecular mechanism of CRNDE in NSCLC progression remains largely unknown.

Material/Methods: qRT-PCR assay was performed to detect the expression levels of CRNDE, miR-641, and cyclin-dependent kinase 6 (CDK6) in NSCLC. Western blot assay was employed to assess CDK6 protein level in treated NSCLC cells. si-CRNDE#1, si-CRNDE#2, miR-641 mimics, miR-641 inhibitors, or Vector-CDK6 were transfected into NSCLC cells to change the expression levels of CRNDE, miR-641, or CDK6. Dual-luciferase reporter assay was performed to validate the direct interrelated miRNA of CRNDE and the potential target of miR-641. MTT and flow cytometry assays were performed to assess the capacities of cell proliferation and apoptosis, respectively.

Results: CRNDE level was upregulated in NSCLC, and its knockdown suppressed NSCLC cells proliferation and enhanced apoptosis, whereas miR-641 antagonized the regulatory effect of CRNDE knockdown by directly binding to CRNDE. Moreover, CDK6 was a target of miR-641 and miR-641 exerted anti-proliferation and pro-apoptosis effects through CDK6.

Conclusions: CRNDE promoted proliferation and inhibited apoptosis of NSCLC cells at least in part by regulating the miR-641/CDK6 axis, suggesting that CRNDE is a potential therapeutic target for NSCLC treatment.

MeSH Keywords: Apoptosis • Carcinoma, Non-Small-Cell Lung • Cell Proliferation • Cyclin-Dependent Kinase 6 • MicroRNAs • RNA, Long Noncoding

Full-text PDF: https://www.medscimonit.com/abstract/index/idArt/913420

📄 3294   🗐 1   📊 6   📚 37

Background

Lung cancer, the most common malignancy, is a predominant cause of cancer-related deaths worldwide [1]. Non-small-cell lung cancer (NSCLC) accounts for 85–90% of lung cancer; it has been increasing in frequency over the last decade and the 5-year survival rate is only 15% [2]. The low survival rate in NSCLC patients is mainly due to the limited efficacy of treatments in advanced disease and poor early diagnosis [1]. Therefore, it is very important to explore novel biomarkers for early diagnosis and treatment.

Long non-coding RNAs (lncRNAs), which are functionally defined as transcripts >200 nt in length with no significant protein-coding potential, have been demonstrated to recruit regulatory complexes via RNA-protein interactions to interpose nearby genes expression [3,4]. Some lncRNAs have been proposed to be involved in a series of pathophysiological processes [5]. Accumulating evidence shows that lncRNAs drive many cancer phenotypes and play pivotal roles in the tumorigenesis and progression of cancers [6,7]. The lncRNA Colorectal Neoplasia Differentially Expressed (CRNDE) gene is located on chromosome 16 and was initially found to be elevated in colorectal cancer [8]. Subsequent reports showed that CRNDE was involved in the molecular pathology of tumorigenesis in some cancers, such as renal cell carcinoma [9], colorectal cancer [10], and multiple myeloma [11]. Moreover, CRNDE overexpression was reported to enhance NSCLC cell proliferation by regulating PI3K/AKT signaling, highlighting its role as an oncogene and potential therapeutic target in NSCLC [12]. Nevertheless, the molecular mechanism of CRNDE in NSCLC progression remains largely unknown.

MicroRNAs (miRNAs), a class of non-coding transcripts 18–23 nt in length, function as regulators of gene expression and thus participate in a series of pathophysiology processes [13]. By base-pairing to the 3' untranslated regions (3'-UTR) of target mRNAs, miRNAs lead to inhibition of translation or degradation of mRNA [14]. Accumulating evidence shows that miRNAs dysregulation is one of the most important factors contributing to the tumorigenesis and progression of many malignancies [15]. Several miRNAs have been found to be involved in NSCLC progression, such as miR-221 and miR-222, which shows tumor-suppressive functions [16], miR-21, which enhances tumor growth [17], and miR-328, which is associated with tumor metastasis [18]. In this study, CRNDE expression was upregulated and CRNDE knockdown suppressed proliferation and enhanced apoptosis in the NSCLC cell line. Moreover, we found that CRNDE promotes proliferation and inhibits apoptosis of NSCLC cells, at least partly through regulating the miR-641/cyclin-dependent kinase 6 (CDK6) axis.

Material and Methods

Clinical specimen collection

A total of 40 NSCLC patients underwent radical excision at Shanxi Provincial Cancer Hospital between March 2011 and November 2011. The following information was collected: age, gender, smoking history, tumor size, TNM stage, and lymph node metastasis (Table 1). The latest follow-up was updated in August 2016, and the median follow-up for overall survival was 50.2 months for patients who remained alive at the time of analysis. Follow-up information was obtained from patients' medical records and overall survival was analyzed.

We collected and stored 40 pairs of NSCLC tissues and corresponding non-cancerous lung tissues in RNAlater (Qiagen, Hilden, Germany) at −80°C. Prior written informed consent was provided by 40 patients, and this study was approved by the Bioethics Committee of Shanxi Provincial Cancer Hospital.

Cell culture

The human bronchial epithelial cell line 16HBE and 4 NSCLC cell lines (H1299, SPC-A1, PC-9, and SK-MES-1) were purchased from the American Tissue Culture Collection (ATCC, Manassas, VA). All cells were maintained in RPMI-1640 medium (Gibco, Rockville, MO) containing 10% heat-inactivated fetal calf serum (HyClone, Cramlington, UK), 100 units/ml penicillin (Sigma-Aldrich, St. Louis, MO), and 100 μg/ml streptomycin (Sigma-Aldrich) at 37°C in a 5% CO_2 humidified incubator. All experiments were carried out using cells in logarithmic phase.

Cell transfection

Modified CRNDE and CDK6 overexpression plasmids (Vector-CRNDE and Vector-CDK6) were commercially constructed by Sigma-Aldrich, and Vector-NC was used as the negative control. Cells were seeded in culture flasks for 24 h, and then were transfected with 50 nmol of CRNDE small interfering RNA (si-CRNDE#1 5'-GUCACGCAGAAGAAGGUUAUT-3' and si-CRNDE#2 5'-GAGUGCUAGUUCUCUUGUAUT-3') or negative control si-NC (5'-UUCUCCGAACGUGUCACGUUT-3', GenePharma, Shanghai, China), 100 nmol of miR-641 mimics or control NC mimics (GenePharma), 100 nmol of miR-641 inhibitors or NC inhibitors (GenePharma), 10 μg of Vector-CRNDE, or Vector-CDK6 using the transfection reagent GeneJammer (Stratagene, Frampton, UK) according to the instructions of the manufacturers.

Real-time quantitative PCR (qRT-PCR)

Total RNA was obtained from NSCLC tissues and cells with the miRVana RNA isolation kit (Ambion, Huntingdon, UK)

Table 1. Correlation of CRNDE expression with clinicopathological features of non-small cell lung cancer patients.

Factor	Number	CRNDE expression			P
		Low	High	(mean ±SD)	
Age (y)					0.124
<60	16	10	6	1.332±0.103	
≥60	24	10	14	1.190±0.070	
Gender					0.128
Male	25	10	15	1.234±0.080	
Female	15	10	5	1.254±0.082	
Smoking history					0.108
Yes	25	11	14	1.385±0.109	
No	15	9	6	1.163±0.064	
Tumor size (cm)					0.002**
<3	18	13	5	1.096±0.100	
≥3	22	7	15	1.370±0.060	
TNM stage					0.001**
I–II	29	19	10	1.135±0.065	
III–IV	11	1	10	1.541±0.078	
Lymph node metastasis					0.014*
Yes	22	8	14	1.370±0.060	
No	18	12	6	1.095±0.100	

* $P<0.05$ and ** $P<0.01$ were considered significantly significant.

following the manufacturer's directions. Then, the integrity of RNA was detected using an Agilent BioAnalyzer 2100 (Agilent, Palo Alto, CA). RNA was reverse transcribed to cDNA with a SuperScript™ II Reverse Transcriptase Kit (Thermo Fisher Scientific, Bremen, Germany). qRT-PCR reactions were performed using Fast SYBR Green One-Step qRT-PCR Kit (Applied Biosystems, Waltham, MA) on a 7900HT Sequence Detection System (Applied Biosystems). GAPDH or U6 served as normalization controls. The comparative C_T method ($2^{-\Delta\Delta CT}$) was used to quantify the gene expression. The reactions were incubated in a 96-well plate at 94°C for 10 min, followed by 40 cycles of 94°C for 15 s and 70°C for 1 min. Primers were:
CRNDE: 5'-GAGGACGTGCTGGGGCT-3' (forward) and
5'-CTGAGTCCATGTCCCGAATC-3' (reverse);
CDK6: 5'-TGGAGACCTTCGAGCACC-3' (forward) and
5'-CACTCCAGGCTCTGGAACTT-3' (reverse);
GAPDH: 5'-GGTGGCAGAGGCCTTTG-3' (forward) and
5'-TGCCCATTTAGCATCTCCTT-3' (reverse);
U6: 5'-CGCTTCGGCAGCACATATAC-3' (forward) and
5'-TTCACGAATTTGCGTGTCAT-3' (reverse).

Cell proliferation assay

MTT assay was used to detect the cell proliferation ability. In brief, cells were seeded into culture plates and then transfected with oligonucleotides or plasmids. At 12 h, 24 h, 48 h, 72 h, and 96 h of transfection, 20 µl of MTT solution (2.5 mg/ml, Promega, Madison, WI) was added to each well, followed by incubation at 37°C for 4 h. Afterwards, the MTT solution was removed and 100 µl of dimethyl sulphoxide (DMSO, Applied Biosystems) was added to each well, followed by the measurement of optical density (OD) at a wavelength of 490 nm using a microplate reader (Bio-Tek Instruments, Inc., Winooski, VT).

Flow cytometry analysis

Flow cytometric method was performed to measure cell apoptosis using an Annexin V-FITC Apoptosis Detection Kit (Invitrogen, Waltham, MA) according to the manufacturers' directions. Briefly, at 48-h transfection, cells were collected and washed with pre-cooled PBS. After that, cells were resuspended in binding buffer containing Annexin V-FITC and propidium iodide, followed by the determination of fluorescence using a flow cytometer (FACSCalibur, Becton Dickinson, Franklin Lakes, NJ).
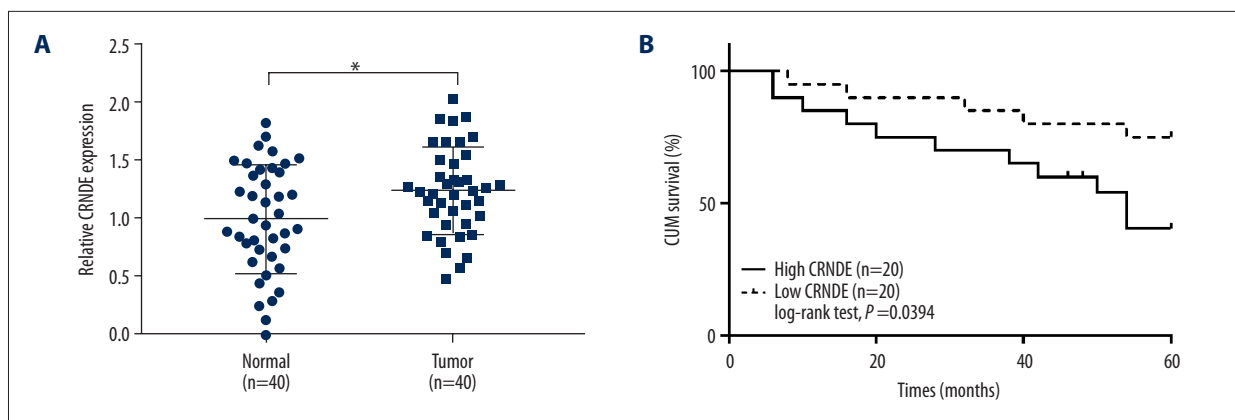
Figure 1. Upregulation of CRNDE level in NSCLC tissues. (**A**) qRT-PCR assay of CRNDE level in 40 pairs of NSCLC tissues and corresponding non-cancerous tissues. (**B**) Kaplan-Meier method and log-rank test were used to evaluate the association between CRNDE level and NSCLC patient prognosis in 40 NSCLC patients in low- and high-risk groups based on CRNDE expression. * P<0.05 vs. normal.

Subcellular fractionation

The isolation of nuclear and cytoplasm fractions was performed using the Cytoplasmic and Nuclear RNA Purification Kit (Norgen, Thorold, ON, Canada). Then, the expression levels of GAPDH, U6, and CRNDE were measured in the nuclear and cytoplasm fractions of H1299 and SPC-A1 cells using qRT-PCR assays, respectively.

Dual-luciferase reporter assay

LncBase Predicted v.2 software (*http://carolina.imis.athena-innovation.gr*) was used to predict the target miRNAs of CRNDE, and TargetScan software (*http://www.targetscan.org/vert_71/*) was used to predict the potential targets of miR-641. Partial sequences of the CRNDE and CDK6 3'-UTR (containing putative complementary sites with miR-641) were inserted downstream of the luciferase-coding sequence in the pMIR-REPORT luciferase vector (Promega). Mutations were introduced into the miRNA-binding sites by using the GeneArt™ Site-Directed Mutagenesis System (Invitrogen). We transfected 500 ng of wild-type or mutant-type reporter vector into cells, together with 100 nmol of miR-641 mimics or miR-641 inhibitors. After 24 h, cells were lysed and the relative luciferase activity was evaluated with the Dual-Luciferase Reporter Assay System (Promega).

Western blot

Protein samples were obtained from transfected cells by using RIPA buffer (Taraka, Beijing, China) containing a protease inhibitor cocktail (Sigma-Aldrich). The equivalent aliquots of proteins were electrophoresed in 12% SDS-polyacrylamide gels and then eletrophoretically transferred to PVDF membranes (Millipore, Billerica, MA). After blocking with 5% non-fat

milk in TBST, the membranes were incubated with anti-CDK6 (1: 2000, Cell Signaling Technology, Danvers, MA) and anti-GAPDH (1: 2500, Cell Signaling Technology) overnight. After washing in TBST, the membranes were then probed with horseradish peroxidase-conjugated secondary antibody (1: 2000, Jackson ImmunoResearch, PA). Immunoreactivity signals were visualized by an echochemiluminescence detection system (GE Healthcare Technologies, Waukesha, WI).

Statistical analysis

All data are expressed as the mean ± s.d. The paired *t* test, Mann-Whitney U test, and one-way analysis of variance (ANOVA) were used to assess significant differences between groups. The Kaplan-Meier method was used to estimate overall survival and the log-rank test was used to analyze difference in survival between 2 groups. *P*-values <0.05 were considered to be statistically significant.

Results

Upregulation of CRNDE level in NSCLC tissues

Initially, qRT-PCR assay was used to observe CRNDE level in 40 pairs of NSCLC tissues and corresponding non-cancerous tissues. These data revealed that CRNDE expression was highly upregulated in NSCLC tissues in comparison to corresponding controls (Figure 1A). To confirm the association between CRNDE expression level and NSCLC patient prognosis, Kaplan-Meier method and log-rank test were performed. The Kaplan-Meier survival curves grouped according to the median value of CRNDE expression level demonstrated that patients (n=20) with high CRNDE expression had a remarkably lower survival rate than those (n=20) with low CRNDE expression
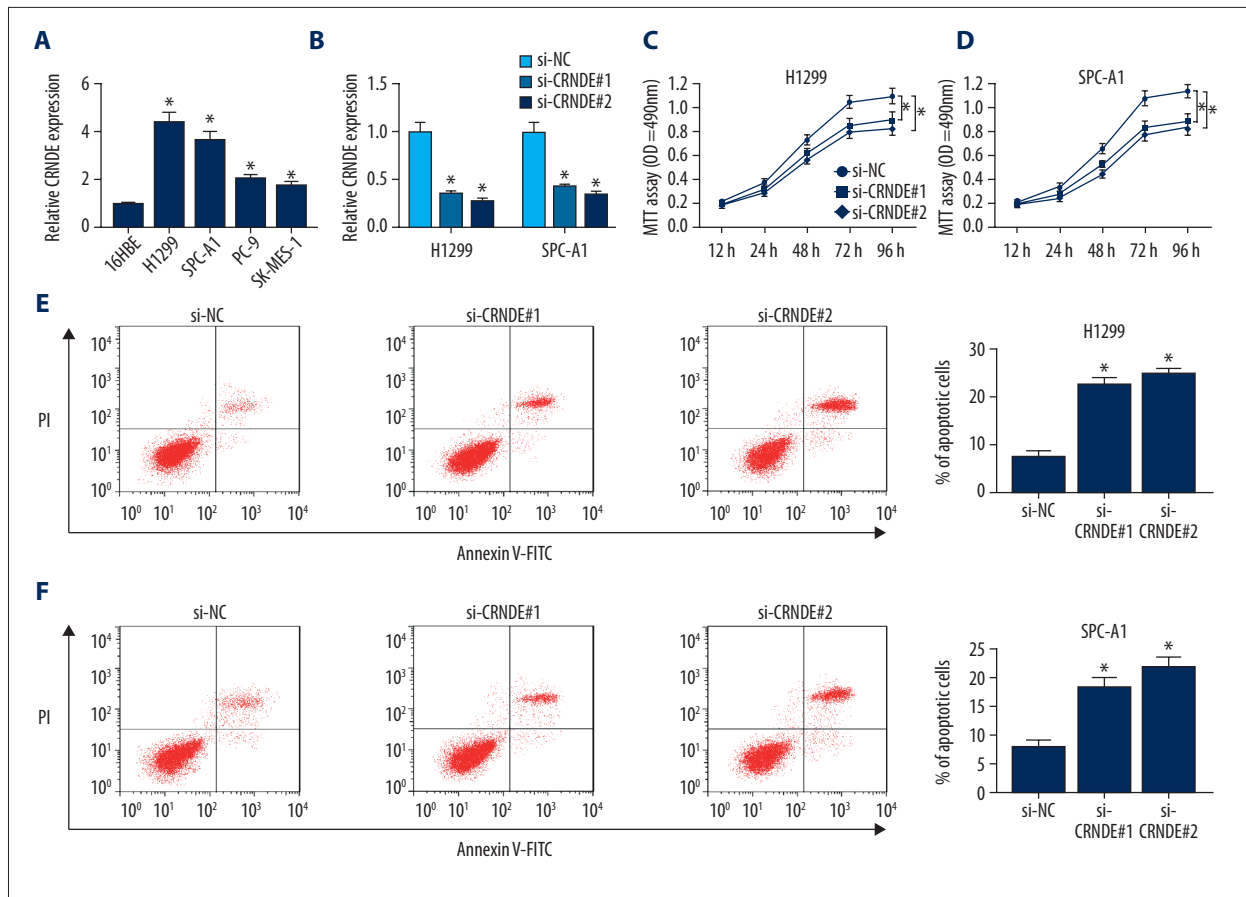
Figure 2. Knockdown of CRNDE suppressed the proliferation and enhanced apoptosis in NSCLC cell lines. (**A**). qRT-PCR of CRNDE expression in human bronchial epithelial cells (16HBE) and NSCLC cell lines (H1299, SPC-A1, PC-9, and SK-MES-1). H1299 and SPC-A1 cells were transfected with si-CRNDE#1 or si-CRNDE#2, followed by qRT-PCR assay of CRNDE expression (**B**), MTT assay of cell proliferation ability (**C, D**), and flow cytometry analysis of cell apoptosis capacity (**E, F**). * $P<0.05$ *vs.* respective control.

(log-rank test, Figure 1B). All these results suggest that upregulated CRNDE expression plays a key role in NSCLC progression.

Association between CRNDE level and clinical features

To investigate the function of CRNDE in NSCLC progression, the correlation between CRNDE and clinical characteristics was assessed. As presented in Table 1, there were significant differences in CRNDE expression for these characteristics, including tumor size (P=0.002), TNM stage (P=0.001), and lymph node metastasis (P=0.014), whereas no significant difference was found in Age (P=0.124), Gender (P=0.128), or Smoking history (P=0.108). All these data indicate that CRNDE level is significantly correlated with tumor size, TNM stage, and lymph node metastasis.

Knockdown of CRNDE suppressed the proliferation and enhanced apoptosis in NSCLC cell lines

Then, we investigated the expression of CRNDE in a series of human bronchial epithelial cells and NSCLC cell lines. Compared with negative control, CRNDE expression was highly elevated in NSCLC cell lines (Figure 2A). To explore the function of CRNDE in NSCLC progression, we manipulated CRNDE expression by transfecting CRNDE small interfering RNAs (si-CRNDE#1 and si-CRNDE#2) into NSCLC cell lines (H1299 and SPC-A1). As shown in Figure 2B, the CRNDE level was significantly attenuated by introduction of si-CRNDE#1 or si-CRNDE#2 into H1299 and SPC-A1 cells (Figure 2B). Subsequently, MTT assay and flow cytometry data showed that the capacity of cell proliferation was markedly inhibited (Figure 2C, 2D), whereas cell apoptosis was highly promoted (Figure 2E, 2F) by CRNDE depletion in H1299 and SPC-A1 cells. Taken together, these observations indicate that CRNDE knockdown represses NSCLC progression *in vitro*, thereby acting as a potential therapeutic agent.
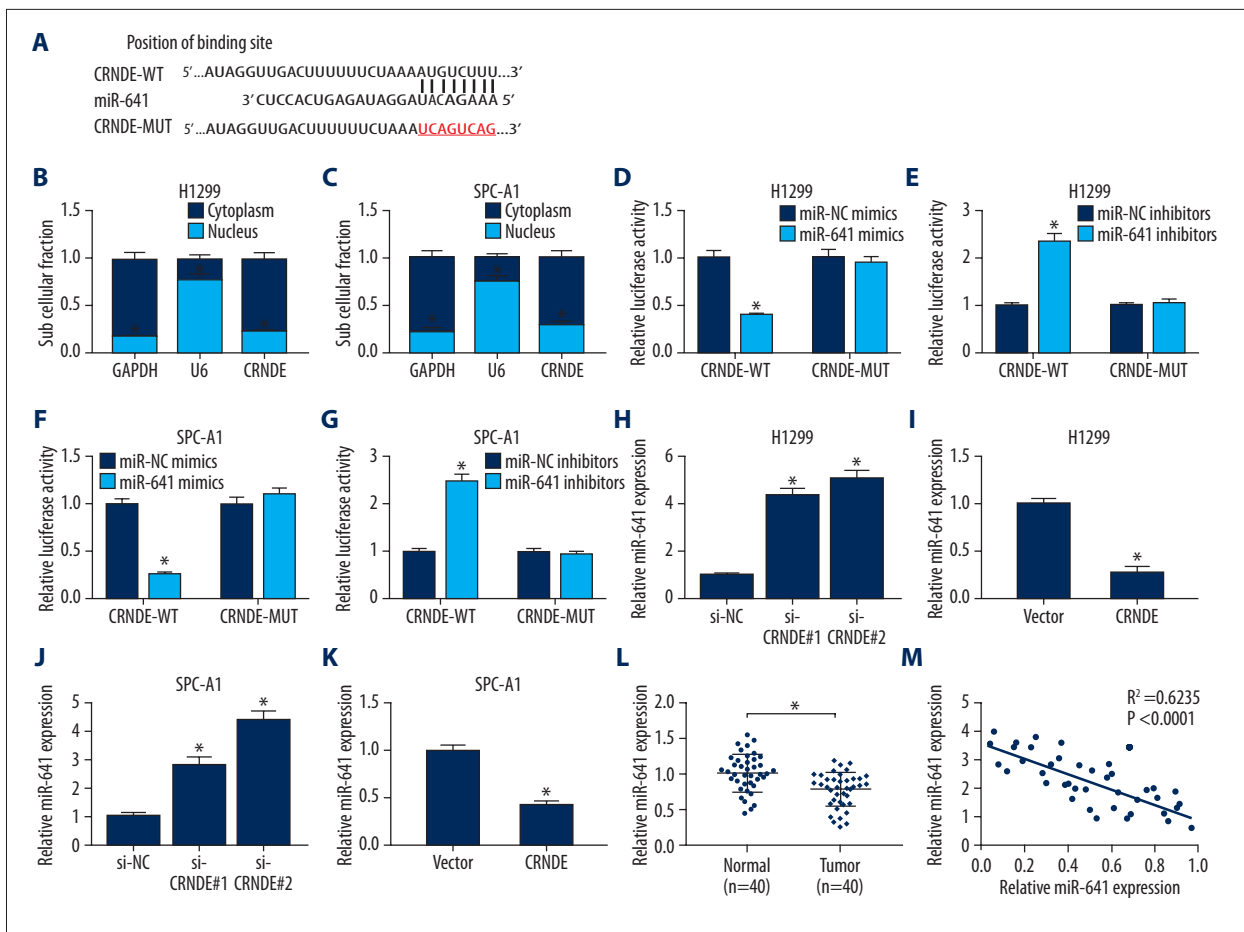
Figure 3. CRNDE repressed miR-641 expression in NSCLC cell lines by direct interaction. (**A**) Putative binding site of miR-641 on the CRNDE and the mutation in the predicted seed region. CRNDE levels were measured in the nuclear and cytoplasm fractions of H1299 (**B**) and SPC-A1 (**C**) cells using qRT-PCR assays. Dual-luciferase reporter assays were used to assess H1299 cells (**D, E**) and SPC-A1 cells (**F, G**) co-transfected with CRNDE-WT or CRNDE-MUT and miR-NC mimics, miR-641 mimics, miR-NC inhibitors, or miR-641 inhibitors. si-CRNDE#1, si-CRNDE#2 or Vector-CRNDE were transfected into H1299 cells (**H, I**) and SPC-A1 cells (**J, K**), followed by the assessment of miR-641 by qRT-PCR assay. (**L**) qRT-PCR assay of miR-641 expression in NSCLC tissues and normal tissues. (**M**) The correlation between CRNDE and miR-641 expression was detected in NSCLC tissues. * *P*<0.05 *vs.* corresponding control.

CRNDE directly bound to miR-641 and repressed miR-641 expression

To further determine the molecular mechanism of CRNDE in NSCLC progression, LncBase Predicted v.2 software was used to predict the targets of CRNDE. Among these potential targets, miR-641 was chosen for further study because it has been validated as a tumor suppressor in NSCLC [19]. The predicted data revealed that CRNDE contained 8 potential complementary bases with miR-641 (Figure 3A). Further, cellular fractionation results revealed that CRNDE was substantially enriched in the cytoplasmic fraction of H1299 and SPC-A1 cells (Figure 3B, 3C). Then, dual-luciferase reporter assay was used to validate whether CRNDE was associated with miR-641. Wild-type and mutant-type CRNDE luciferase vectors (CRNDE-WT and CRNDE-MUT) were constructed and co-transfected into H1299 and SPC-A1 cells with miR-NC mimics, miR-641 mimics, miR-NC inhibitors, or miR-641 inhibitors. The results revealed that the luciferase activity of CRNDE-WT was highly repressed by upregulated miR-641 in H1299 and SPC-A1 cells, but it was markedly enhanced by miR-641 knockdown (Figure 3D–3G). However, there was no change in the luciferase activity of CRNDE-MUT when co-transfected with miR-641 mimics or miR-641 inhibitors (Figure 3D–3G).

Next, we explored whether miR-641 expression was regulated by CRNDE in H1299 and SPC-A1 cells. The data showed that, compared with the control, miR-641 expression was increased almost 4-fold in si-CRNDE#1 H1299 cells and 5-fold in si-CRNDE#2 H1299 cells (Figure 3H), while miR-641 expression
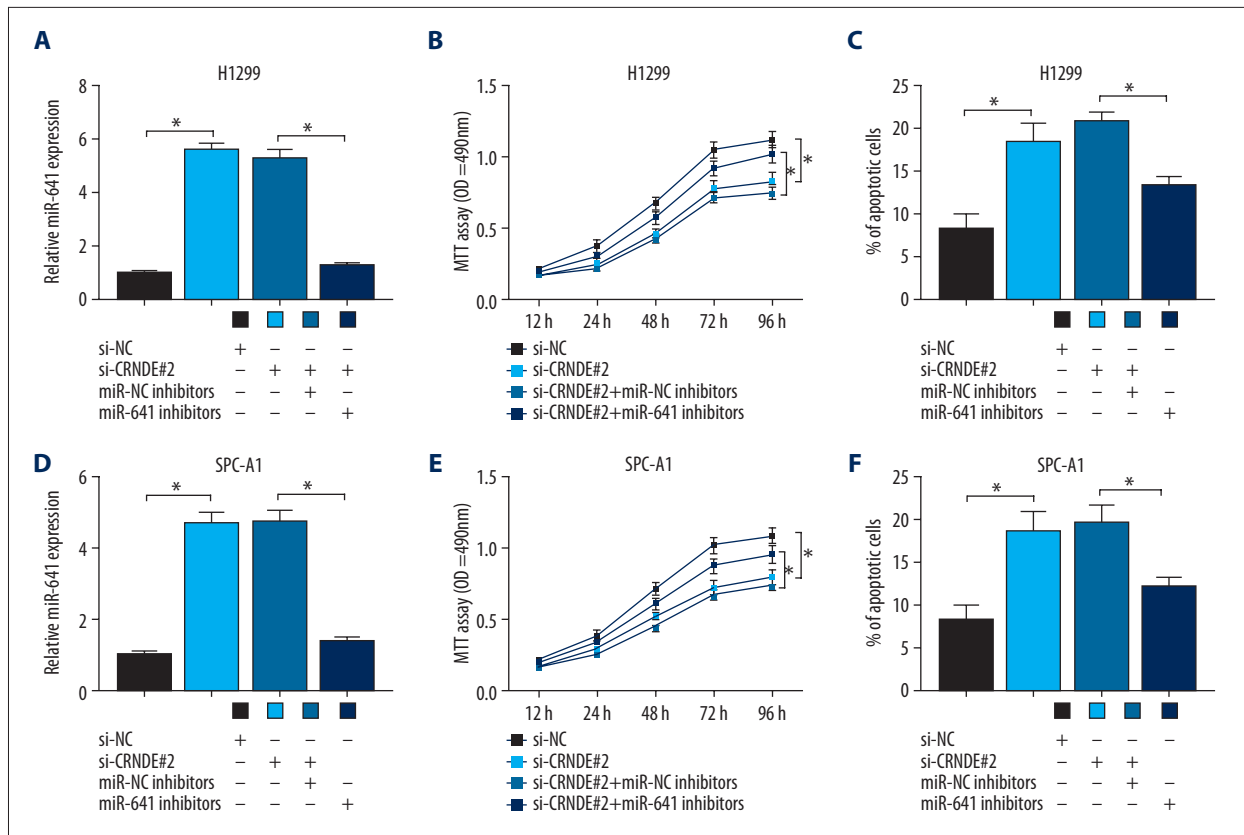
Figure 4. The restoration of miR-641 level reduced the si-CRNDE#2-mediated anti-proliferation and pro-apoptosis effects on NSCLC cells. si-NC, si-CRNDE#2, si-CRNDE#2+miR-NC inhibitors, or si-CRNDE#2+miR-641 inhibitors were transfected into H1299 and SPC-A1 cells, followed by measurement of miR-641 expression (**A, D**), cell proliferation ability (**B, E**), and apoptosis capacity (**C, F**). * *P*<0.05 *vs.* si-NC or si-CRNDE#2+miR-NC inhibitors.

in Vector-CRNDE H1299 cells was nearly 4 times lower in Vector cells (Figure 3I). In parallel, miR-641 level was about 3-fold higher in si-CRNDE#1 SPC-A1 cells and 4-fold higher in si-CRNDE#2 SPC-A1 cells compared to the control (Figure 3J), while in Vector-CRNDE SPC-A1 cells it was approximately 2 times lower than in Vector cells (Figure 3K). Then, we measured miR-641 expression level and the association between CRNDE and miR-641 expression in NSCLC tissues. Interestingly, qRT-PCR assay showed that the miR-641 level was greatly reduced compared with normal tissues (Figure 3L). Moreover, the endogenous miR-641 level was negatively correlated with CRNDE in NSCLC tissues (Figure 3M). All these findings suggest that CRNDE represses miR-641 expression by binding to miR-641.

The si-CRNDE-mediated regulatory effect was weakened by miR-641 level restoration in NSCLC cell lines

To determine if CRNDE knockdown exerting anti-proliferation and pro-apoptosis function was mediated by miR-641, si-CRNDE#2 was transfected into H1299 and SPC-A1 cells together with miR-641 inhibitors. qRT-PCR assay revealed, that compared with the control, the enhancement effect of

si-CRNDE#2 on miR-641 expression was significantly weakened by co-transfection with miR-641 inhibitors (Figure 4A, 4D). Subsequent functional experiments demonstrated that the si-CRNDE#2-mediated anti-proliferation and pro-apoptosis effect was dramatically abrogated by the restoration of miR-641 expression in H1299 (Figure 4B, 4C) and SPC-A1 cells (Figure 4E, 4F). All these data suggest that CRNDE is involved in NSCLC progression, at least partly through miR-641.

CDK6 was a target gene of miR-641

Subsequently, we used TargetScan computational software to predict the potential target genes of miR-641. Intriguingly, there were 7 potential complementary bases in the 3'-UTR of CDK6 mRNA and miR-641 (Figure 5A). To verify the prediction, CDK6-3'-UTR (containing putative complementary sites with miR-641) was cloned into pMIR-REPORT luciferase vector to generate wild-type CDK6 luciferase reporter vector (CDK6-WT). In parallel, a mutated seed site in CDK6-3'-UTR was also cloned into pMIR-REPORT luciferase vector to generate mutant-type CDK6 luciferase reporter vector (CDK6-MUT). Transfection of CDK6-WT into H1299 and SPC-A1 cells showed that the
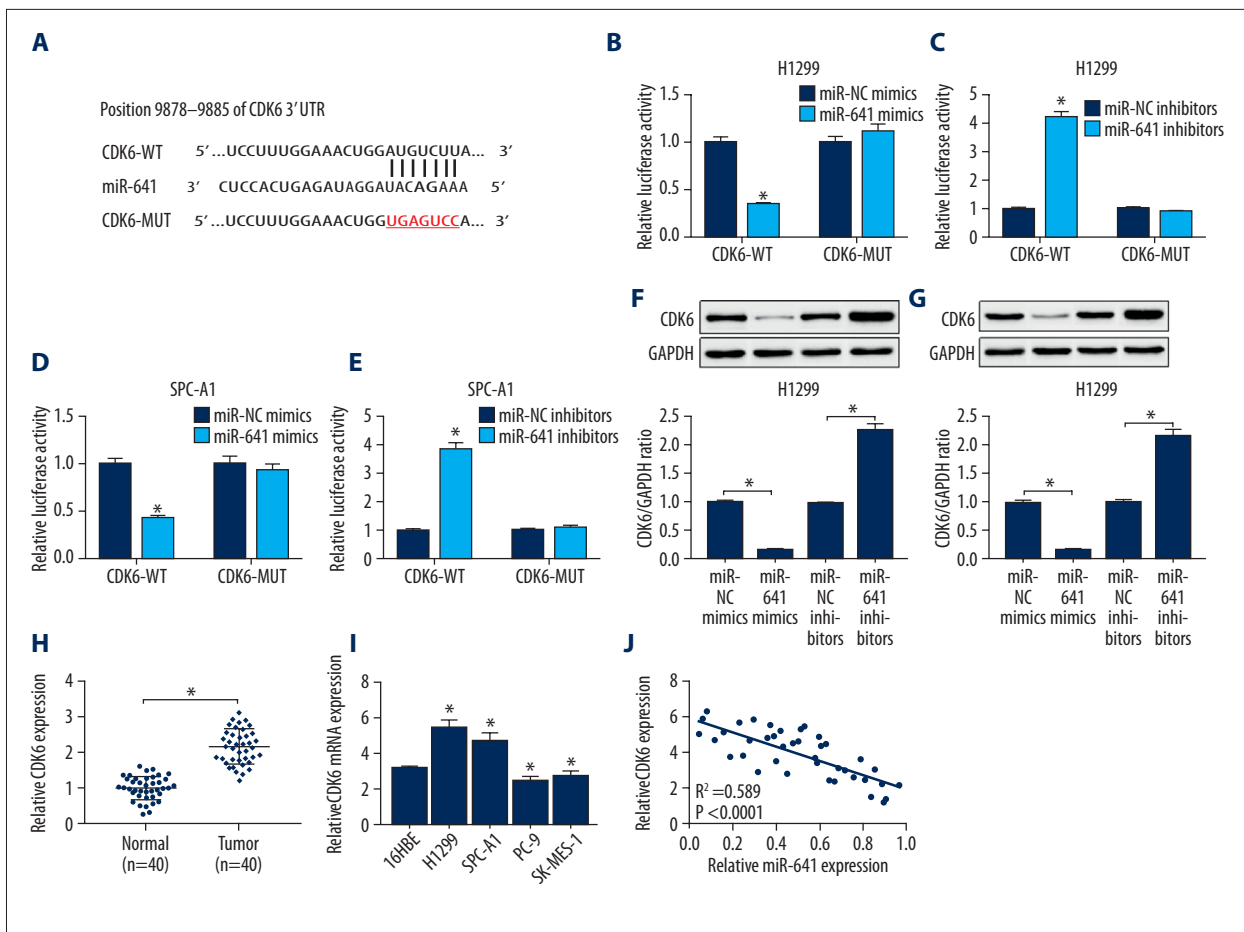
Figure 5. CDK6 is a direct target of miR-641. (**A**) Putative binding site of miR-641 on CDK6 and the mutation in the predicted seed region. Dual-luciferase reporter assays were used to assess H1299 cells (**B, C**) and SPC-A1 cells (**D, E**) co-transfected with CDK6-WT or CDK6-MUT and miR-NC mimics, miR-641 mimics, miR-NC inhibitors, or miR-641 inhibitors. miR-NC mimics, miR-641 mimics, miR-NC inhibitors, or miR-641 inhibitors were transfected into H1299 cells (**F**) and SPC-A1 cells (**G**), followed by determination of CDK6 protein level by Western blot analysis. qRT-PCR assay of CDK6 expression in NSCLC tissues and normal tissues (**H**), NSCLC cell lines and 16HBE (**I**). (**J**) The correlation between CRNDE and miR-641 expression was assessed in NSCLC tissues. * $P<0.05$ *vs.* respective control.

luciferase activity of CDK6-WT was inversely correlated with miR-641 expression level (Figure 5B–5E), whereas the effect of miR-641 on luciferase activity was abolished when putative seed sequences were mutated (Figure 5B–5E).

Next, to explore whether miR-641 regulates CDK6 expression, miR-641 mimics or miR-641 inhibitors were transfected into H1299 and SPC-A1 cells. These results showed that CDK6 expression was almost 7 times lower in miR-641 mimics H1299 cells and 2 times lower in miR-641 inhibitor H1299 cells compared with corresponding control (Figure 5F). In parallel, compared to the respective controls, CDK6 expression was about 6 times lower in miR-641 mimics SPC-A1 cells and 2 times lower in miR-641 inhibitor SPC-A1 cells (Figure 5G). Then, we assessed CDK6 expression level in NSCLC tissues and cell lines, and the association between CDK6 and miR-641 level in NSCLC

tissues. Interestingly, these results showed that CDK6 levels were higher in NSCLC tissues and cell lines than in normal controls (Figure 5H, 5I). Moreover, CDK6 expression was inversely correlated with miR-641 level in NSCLC tissues (Figure 5J). These results indicate that CDK6 is a direct target of miR-641.

miR-641 exerts anti-proliferation and pro-apoptosis effects through targeting CDK6 in NSCLC cell lines

It was previously reported that miR-641 represses cell proliferation and enhances apoptosis by targeting PDCD4 in NSCLC cells [19]. Here, we investigated whether miR-641 regulates NSCLC progression through targeting CDK6. H1299 and SPC-A1 cells were transfected with miR-641 mimics alone or together with CDK6 overexpression vector (Vector-CDK6), followed by the determination of CDK6 expression. As shown
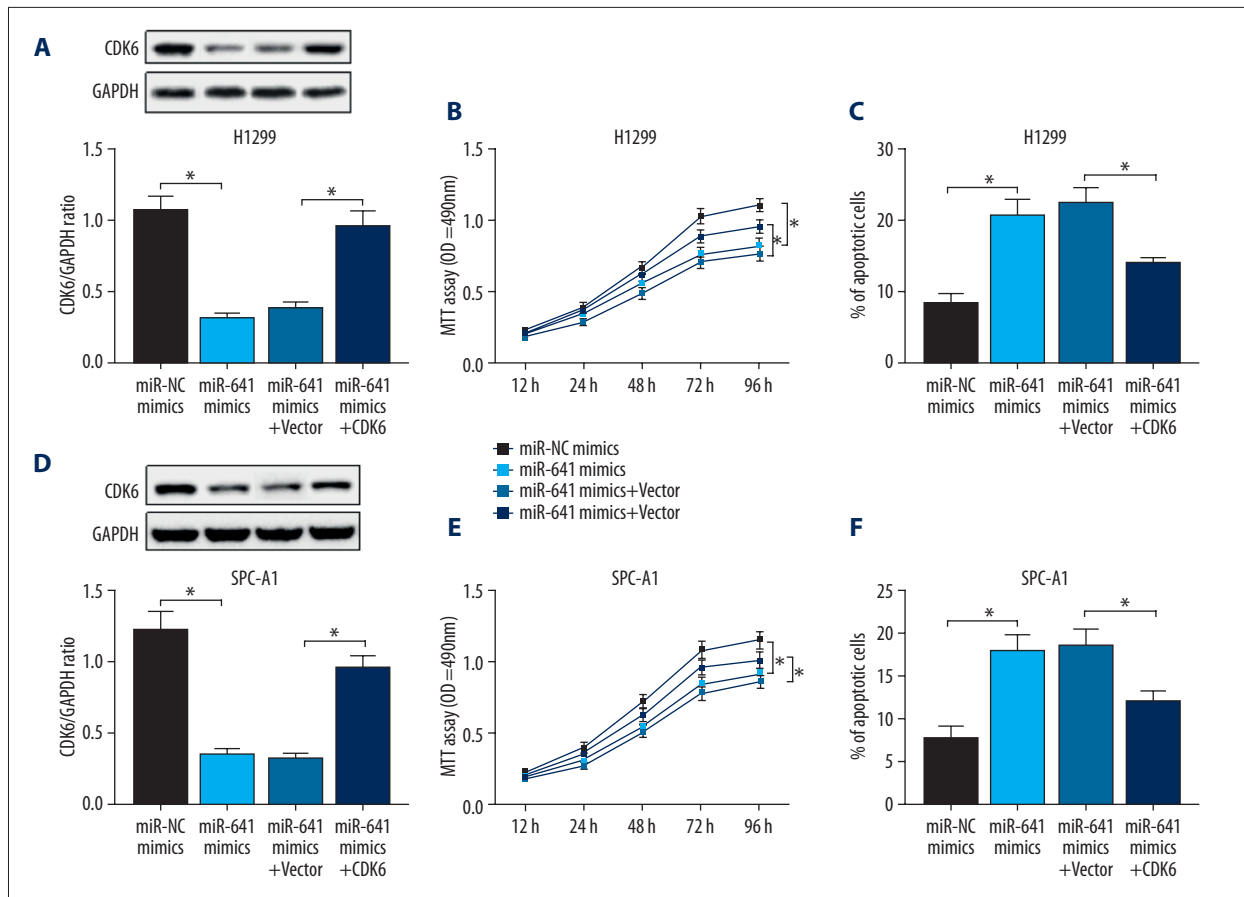
Figure 6. miR-641 exerts anti-proliferation and pro-apoptosis effects through targeting CDK6 in NSCLC cell lines. miR-NC mimics, miR-641 mimics, miR-641 mimics+Vector-NC, or miR-641 mimics+Vector-CDK6 were transfected into H1299 and SPC-A1 cells, followed by the detection of CDK6 expression (**A, D**), cell proliferation ability (**B, E**), and cell apoptosis capacity (**C, F**). * $P<0.05$ *vs.* miR-NC mimics or miR-641 mimics+vector.

in Figure 6A and 6D, the miR-641-mediated suppression of CDK6 expression was markedly abolished by co-transfection with Vector-CDK6. Further, MTT and flow cytometry assays verified that miR-641 overexpression significantly suppressed cell proliferation and promoted apoptosis (Figure 6B, 6C, 6E, 6F). Nevertheless, the miR-641-mediated regulatory effect on cell proliferation and apoptosis was significantly abrogated by CDK6 expression restoration (Figure 6B, 6C, 6E, 6F). Together, these data suggest that miR-641 suppresses NSCLC progression through targeting CDK6.

Discussion

In recent years, accumulating evidence has suggested that lncRNAs are dysregulated and play key roles in tumorigenesis and tumor progression [6]. Many reports have illuminated the wide involvement of lncRNAs in NSCLC [7]. For example, the upregulation of AFAP1-AS1 is associated with NSCLC patient prognosis [20]. PVT1 is upregulated in NSCLC tissues

and cells, which is correlated with histological grade and lymph node metastasis [21]. UCA1 overexpression was reported to accelerate NSCLC cells proliferation and colony formation by sponging miR-193a-3p, highlighting its role as a potential oncogenic gene in NSCLC [22]. Conversely, downregulated SPRY4-IT1 was demonstrated to be correlated with a poor prognosis of NSCLC [23]. MEG3 was also downregulated in NSCLC tissues and regulated proliferation and apoptosis in NSCLC cells through p53 activation [24]. Consistent with the findings of Liu et al. [12], we verified that CRNDE level was elevated in NSCLC tissues and cell lines, and CRNDE knockdown repressed NSCLC progression *in vitro*, thereby acting as a potential oncogene in NSCLC.

The competing endogenous RNA (ceRNA) hypothesis proposes that a series of lncRNAs function as molecular sponges of miRNAs to regulate target mRNAs expression, and thus play important roles in the tumorigenic and developmental process [25]. Thus, LncBase Predicted v.2 software was used to predict the target miRNAs of CRNDE. Among these candidates, miR-641

This work is licensed under Creative Common Attribution-
NonCommercial-NoDerivatives 4.0 International (CC BY-NC-ND 4.0)

2753

Indexed in: [Current Contents/Clinical Medicine] [SCI Expanded] [ISI Alerting System]
[ISI Journals Master List] [Index Medicus/MEDLINE] [EMBASE/Excerpta Medica]
[Chemical Abstracts/CAS]

was chosen for further study. miR-641, located in chromosome 19q13.2 near the amplicon, has been reported to play pivotal roles in the tumorigenesis and progression of cancers. For instance, miR-641 level was decreased in hematological malignancy cell lines [26]. miR-641 is also one of the miRNAs that are altered in hepatocellular carcinoma, predicting a novel therapeutic agent [27]. Moreover, miR-641 was demonstrated to be a tumor suppressor in glioblastoma multiforme through inactivating the PI3K/AKT pathway via targeting AKT2 [28]. In parallel, the miR-641-activated MAPK pathway, by regulating tumor suppressor NF1 and cooperating with AKT2, has a role as an oncomiR in human cancer [29]. Recently, it was reported that miR-641 functions as a tumor suppressor in NSCLC through targeting MDM2 and PDCD4 [30]. Additionally, upregulation of miR-641 expression contributes to development of erlotinib resistance through regulating the NF1/ERK signaling pathway in NSCLC [31]. In the present study, we found that CRNDE acts as a molecular sponge of miR-641, and the regulatory effect of CRNDE depletion was abated by miR-641 level restoration in NSCLC cell lines. All these results suggest that CRNDE promotes NSCLC progression, at least in part through miR-641.

Subsequently, TargetScan software was used to search for the potential targets of miR-641. Interestingly, the predicted data showed that CDK6 might be a potential target of miR-641. Then, we verified that CDK6 was a direct target of miR-641 and found that miR-641 negatively regulated CDK6 expression. CDK6, detected at chromosome 7q21.2, encodes cyclin-dependent serine-threonine kinases, which play a key role in reacting to mitogenic or pro-proliferative stimuli [32]. Upregulation of CDK6 was identified as a new molecular marker of prognosis in medulloblastoma [33]. CDK6 was also demonstrated to

induce cell-cycle arrest and senescence in neuroblastoma, supporting its role as a therapy for patients with this disease [34]. Moreover, Kikkawa et al. [35] found that miR-504 repressed cell proliferation through targeting CDK6 in hypopharyngeal squamous cell carcinoma. Agirre et al. [36] reported that miR-124a acts as a potential tumor suppressor through directly targeting CDK6-phosphorylation of retinoblastoma (Rb) pathway in acute lymphoblastic leukemia. Interestingly, Zhang et al. [37] found that miR-377 repressed tumor growth *in vitro* through targeting CDK6 in NSCLC. Consistent with these reports, we verified that CDK6 is upregulated in NSCLC tissues and CDK6 is a direct target of miR-641. Moreover, miR-641 exerts its tumor-suppressive effect by targeting CDK6 in NSCLC cell lines.

Conclusions

In conclusion, CRNDE promotes proliferation and inhibits apoptosis in NSCLC cells, at least partly through regulating the miR-641/CDK6 axis, suggesting that CRNDE is a potential therapeutic target for NSCLC treatment.

Conflicts of interest

None.

Ethics approval and consent to participate

Prior written informed consent was provided from all 40 patients, and the study was approved by the Bioethics Committee of Shanxi Provincial Cancer Hospital.

References:

1. Torre LA, Bray F, Siegel RL et al: Global cancer statistics, 2012. Cancer J Clin, 2015; 65: 87–108

2. Gridelli C, Rossi A, Carbone DP et al: Non-small-cell lung cancer. Nat Rev Dis Primers, 2015; 1: 15009

3. Engreitz JM, Haines JE, Perez EM et al: Local regulation of gene expression by lncRNA promoters, transcription and splicing. Nature, 2016; 539: 452–55

4. Wang KC, Yang YW, Liu B et al: A long noncoding RNA maintains active chromatin to coordinate homeotic gene expression. Nature, 2011; 472: 120–24

5. Batista PJ Chang HY: Long noncoding RNAs: Cellular address codes in development and disease. Cell, 2013; 152: 1298–307

6. Schmitt AM Chang HY: Long noncoding RNAs in cancer pathways. Cancer Cell, 2016; 29: 452–63

7. Yang J, Lin J, Liu T et al: Analysis of lncRNA expression profiles in non-small cell lung cancers (NSCLC) and their clinical subtypes. Lung Cancer, 2014; 85: 110–15

8. Graham LD, Pedersen SK, Brown GS et al: Colorectal neoplasia differentially expressed (CRNDE), a novel gene with elevated expression in colorectal adenomas and adenocarcinomas. Genes Cancer, 2011; 2: 829–40

9. Shao K, Shi T, Yang Y et al: Highly expressed lncRNA CRNDE promotes cell proliferation through Wnt/beta-catenin signaling in renal cell carcinoma. Tumour Biol, 2016 [Epub ahead of print]

10. Han P, Li JW, Zhang BM et al: The lncRNA CRNDE promotes colorectal cancer cell proliferation and chemoresistance via miR-181a-5p-mediated regulation of Wnt/beta-catenin signaling. Mol Cancer, 2017; 16: 9

11. Meng YB, He X, Huang YF et al: Long noncoding RNA CRNDE promotes multiple myeloma cell growth by suppressing miR-451. Oncol Res, 2017; 25: 1207–14

12. Liu XX, Xiong HP, Huang JS et al: Highly expressed long non-coding RNA CRNDE promotes cell proliferation through PI3K/AKT signalling in non-small cell lung carcinoma. Clin Exp Pharmacol Physiol, 2017; 44: 895–902

13. Filipowicz W, Bhattacharyya SN Sonenberg N: Mechanisms of post-transcriptional regulation by microRNAs: Are the answers in sight? Nat Rev Genet, 2008; 9: 102–14

14. van Kouwenhove M, Kedde M Agami R: MicroRNA regulation by RNA-binding proteins and its implications for cancer. Nat Rev Cancer, 2011; 11: 644–56

15. Tiberio P, Callari M, Angeloni V et al: Challenges in using circulating miRNAs as cancer biomarkers. Biomed Res Int, 2015; 2015: 731479

16. Yamashita R, Sato M, Kakumu T et al: Growth inhibitory effects of miR-221 and miR-222 in non-small cell lung cancer cells. Cancer Med, 2015; 4: 551–64

17. Zhang JG, Wang JJ, Zhao F et al: MicroRNA-21 (miR-21) represses tumor suppressor PTEN and promotes growth and invasion in non-small cell lung cancer (NSCLC). Clin Chim Acta, 2010; 411: 846–52

18. Arora S, Ranade AR, Tran NL et al: MicroRNA-328 is associated with (non-small) cell lung cancer (NSCLC) brain metastasis and mediates NSCLC migration. Int J Cancer, 2011; 129: 2621–31

19. Zhou J, Li H, Li N et al: MicroRNA-641 inhibits lung cancer cells proliferation, metastasis but promotes apoptosis in cells by targeting PDCD4. Int J Clini Exp Pathol, 2017; 10: 8211–21

20. Deng J, Liang Y, Liu C et al: The up-regulation of long non-coding RNA AFAP1-AS1 is associated with the poor prognosis of NSCLC patients. Biomed Pharmacother, 2015; 75: 8–11

21. Yang YR, Zang SZ, Zhong CL et al: Increased expression of the lncRNA PVT1 promotes tumorigenesis in non-small cell lung cancer. Int J Clin Exp Pathol, 2014; 7: 6929–35

22. Nie W, Ge HJ, Yang XQ et al: LncRNA-UCA1 exerts oncogenic functions in non-small cell lung cancer by targeting miR-193a-3p. Cancer Lett, 2016; 371: 99–106

23. Sun M, Liu XH, Lu KH et al: EZH2-mediated epigenetic suppression of long noncoding RNA SPRY4-IT1 promotes NSCLC cell proliferation and metastasis by affecting the epithelial-mesenchymal transition. Cell Death Dis, 2014; 5: e1298

24. Lu KH, Li W, Liu XH et al: Long non-coding RNA MEG3 inhibits NSCLC cells proliferation and induces apoptosis by affecting p53 expression. BMC Cancer, 2013; 13: 461

25. Yoon JH, Abdelmohsen K, Gorospe M: Functional interactions among microRNAs and long noncoding RNAs. Semin Cell Dev Biol, 2014; 34: 9–14

26. Lawrie CH, Saunders NJ, Soneji S et al: MicroRNA expression in lymphocyte development and malignancy. Leukemia, 2008; 22: 1440–46

27. Zhang CJ Du HJ: Screening key miRNAs for human hepatocellular carcinoma based on miRNA-mRNA functional synergistic network. Neoplasma, 2017; 64: 816–23

28. Hinske LC, Heyn J, Hubner M et al: Intronic miRNA-641 controls its host Gene's pathway PI3K/AKT and this relationship is dysfunctional in glioblastoma multiforme. Biochem Biophys Res Commun, 2017; 489: 477–83

29. Richards EJ, Coppola M, Guo J et al: Abstract B28: MicroRNA-641 activates MAPK by targeting NF1 and cooperates with its host gene AKT2 in human cancer. Cancer Res, 2012; 72: B28

30. Kong Q, Shu N, Li J et al: miR-641 functions as a tumor suppressor by targeting MDM2 in human lung cancer. Oncol Res, 2018; 26: 735–41

31. Chen J, Cui JD, Guo XT et al: Increased expression of miR-641 contributes to erlotinib resistance in non-small-cell lung cancer cells by targeting NF1. Cancer Med, 2018; 7: 1394–403

32. Harbour JW, Luo RX, Dei Santi A et al: Cdk phosphorylation triggers sequential intramolecular interactions that progressively block Rb functions as cells move through G1. Cell, 1999; 98: 859–69

33. Mendrzyk F, Radlwimmer B, Joos S et al: Genomic and protein expression profiling identifies CDK6 as novel independent prognostic marker in medulloblastoma. J Clin Oncol, 2005; 23: 8853–62

34. Rader J, Russell MR, Hart LS et al: Dual CDK4/CDK6 inhibition induces cell-cycle arrest and senescence in neuroblastoma. Clin Cancer Res, 2013; 19: 6173–82

35. Kikkawa N, Kinoshita T, Nohata N et al: microRNA-504 inhibits cancer cell proliferation via targeting CDK6 in hypopharyngeal squamous cell carcinoma. Int J Oncol, 2014; 44: 2085–92

36. Agirre X, Vilas-Zornoza A, Jimenez-Velasco A et al: Epigenetic silencing of the tumor suppressor microRNA Hsa-miR-124a regulates CDK6 expression and confers a poor prognosis in acute lymphoblastic leukemia. Cancer Res, 2009; 69: 4443–53

37. Zhang J, Zhao M, Xue ZQ et al: miR-377 inhibited tumorous behaviors of non-small cell lung cancer through directly targeting CDK6. Eur Rev Med Pharmacol Sci, 2016; 20: 4494–99